16TH EUROPEAN CONFERENCE ON EARTHQUAKE ENGINEERING THESSALONIKI 18 - 21 JUNE 2018

ACCRUAL OF DISPLACEMENTS FOR SLIDING ISOLATORS WITH CURVED SURFACES

Virginio QUAGLINI[1], Paolo DUBINI[2], Emanuele GANDELLI[3]

ABSTRACT

For base-isolated structures, fulfillment of the non-collapse requirement demands that at the ultimate limit state, the ultimate capacity of the isolating devices in terms of strength and deformability is not exceeded.
A criterion for establishing the displacement capacity required by isolation systems, accounting for the effects of both non-seismic and seismic actions, as well as for possible accrual of displacements during the lifetime of the structure, in case of system with poor restoring capability, is provided in the Eurocode 8. However this criterion is rather empirical and its validity for isolation devices endowed with high nonlinear behavior has been never proved in practice.
The study addresses the concern of displacement accrual for sliding isolators with curved surfaces, investigating in a parametric study the effect of a non-seismic offset displacement on the total displacement induced by the design earthquake. Nonlinear History Response Analyses were conducted, accounting for five offset displacements, combined with a wide range of devices and earthquake characteristics. Twenty-five different isolators were obtained from five radii of curvature (from 2200 mm to 5000 mm) and five friction coefficients, covering the design practice. Twenty-four natural ground motion histories were selected from a database according to their predominant period and pulse-like behavior.
The Eurocode provision is checked against the observed data, an improved formulation of the Eurocode's displacement capacity for sliding isolators with curved surfaces is proposed, together with a criterion to evaluate the capability of the devices to provide a seismic response independent of the non-seismic displacement.

Keywords: Isolation; Re-Centering Capability; Displacement Accrual; Curved Surface Slider; Parametric study

1. INTRODUCTION

The re-centering capability, or the ability to return towards the origin at the end of the perturbation, is recognized by the European code on seismic design, or Eurocode 8 (CEN 2004, 2005), as an essential property of base isolation systems. This capability is indeed necessary for the fulfillment of the compliance criteria at the damage limitation and ultimate limit states. Large residual displacements of an isolated structure after the earthquake can affect its serviceability and jeopardize the functionality of the lifelines and the nonstructural elements that cross the isolation plane, like fire protection and weather proofing elements, elevators, etc.; moreover, large residual displacement can impair the capability of the isolating devices to withstand future earthquakes. The re-centering capability assumes a primary importance in situations of seismic sequences characterized by frequent medium-strong intensity ground motions following a strong mainshock after short intervals of time, as recorded also in recent earthquakes (Carydis et al. 2012; Decanini et al. 2000; Di Sarno et al. 2011, 2013; Huang et al. 2008; Motosaka et al. 2012). Since it may be not possible to re-center the isolators before the occurrence of close aftershocks, the possibility that ground motion sequences with such characteristics would produce an accrual of displacements, making the capacity of the isolation system inadequate at the end of the sequence, is of practical concern.

[1]Associate Professor, Department A.B.C., Politecnico di Milano, Milan, Italy, virginio.quaglini@polimi.it
[2]Research Fellow, Department A.B.C., Politecnico di Milano, Milan, Italy, paolo.dubini@polimi.it
[3]Research Fellow, Department A.B.C., Politecnico di Milano, Milan, Italy, emanuele.gandelli@polimi.it

According to Eurocode 8 (CEN, 2005), the isolation system has sufficient re-centering capability when the condition is met

$$\frac{d_m}{d_{rm}} \geq \delta \tag{1}$$

where d_m is the seismic displacement under the design earthquake, d_{rm} is the maximum residual displacement at which the isolating system can be in static equilibrium, and δ a numeric coefficient that counts δ = 0.5. For an isolation system with bilinear force-displacement behavior the maximum residual displacement d_{rm} is given by the ratio between the characteristic strength F_0 and the restoring stiffness K_2 (Figure 1) and depends only on the mechanical properties of the system.

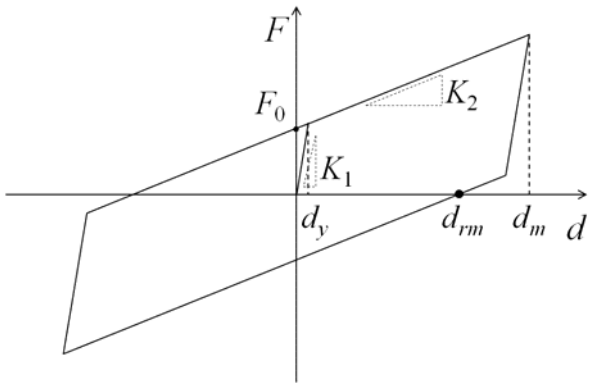

Figure 1. Force – displacement curve of a bilinear hysteretic isolation system. F_0 : characteristic strength, K_1 : elastic stiffness, K_2 : post-yield or restoring stiffness, d_y : yield displacement

Isolation systems satisfying Equation (1) are assumed to have enough restoring capability to prevent the accumulation of displacements during repeated events. In such case, the Eurocode recommends that the horizontal displacement capacity D_i of the i-th isolator of the system shall be designed to satisfy the condition

$$D_i \geq d_{G,i} + \gamma_{IS} \cdot d_{m,i} \tag{2}$$

where $d_{G,i}$ is the displacement of the i-th isolator induced by non-seismic actions, $d_{m,i}$ is the displacement of the isolator induced by the design earthquake, and γ_{IS} is an amplification factor that counts γ_{IS} = 1.2 for buildings and γ_{IS} = 1.5 for bridges (CEN 2005). The basic assumption is that the offset displacement $d_{G,i}$ does not affect the entity of the seismic displacement, and the linear superposition of the effects of non-seismic and seismic actions applies.
On the contrary, isolating systems not satisfying Equation (1) shall be provided with sufficient displacement capacity to accommodate the accrual of residual displacements during the service life of the structure, and the capacity of the i-th isolator is required to satisfy (CEN 2005)

$$D_i \geq d_{G,i} + \gamma_{du} \cdot \rho_d \cdot d_{m,i} \tag{3}$$

where the factor γ_{du} = 1.2 covers the uncertainties in the estimation of the design displacement, and ρ_d accounts for the possible accumulation of residual displacements under a sequence of seismic events occurring before the design earthquake, considered to have the same probability to occur:

$$\rho_d = 1 + 1.35 \frac{1 - \left(d_y / d_m\right)^{0.6}}{1 + 80\left(d_m / d_{rm}\right)^{1.5}} \tag{4}$$

where d_y is the yield displacement of the equivalent bilinear system (Figure 1), and the other quantities have been already defined; for systems with $d_m/d_{rm} > 0.5$ the accumulation of residual displacements is insignificant ($\rho_d < 1.05$).
The code's criteria are mainly based on semi-empirical assumptions, like e.g. effects superposition for re-centering systems, rather than on solid fundamentals, and, above all, they are not supported by exhaustive experimental results. In particular, while their validity has been numerically demonstrated for conventional bilinear hysteretic systems (Katsaras et al. 2008), numerical and experimental studies concluded that the criterion $d_m/d_{rm} > 0.5$ may be not conservative for isolating devices with high damping capacity or characterized by a strong nonlinear behavior, like "flag-shaped" devices comprising self-centering Shape Memory Alloy elements (Cardone 2012), and sliding devices with curved surfaces (Cardone et al. 2015, 2017; Ponzo et al. 2017; Quaglini et al. 2017a).
The sliding isolator with curved surfaces, known as Curved Surface Slider (CSS) or Friction Pendulum System (FPS), introduced in the '80s of the last century (Zayas et al. 1987, 1990), and today is one among the most popular isolation devices worldwide (Martelli et al. 2014). In its basic version, the Curved Surface Slider consists of a concave plate and an articulated slider (Figure 2), and a sliding surface is formed between the slider and the concave plate to accommodate the horizontal displacement of the superstructure. The concave surface provides a restoring force that is proportional to the horizontal displacement, while the friction force developed during the accommodated sliding motion provides the energy dissipation capability, with benefits of reduction in the transmitted lateral force and in the displacement demand. Though improved versions with multiple sliding surfaces have been proposed in recent years, like the Double Concave Surface Slider (Fenz and Constantinou 2006), and the Triple Friction Pendulum (Fenz and Constantinou 2008a, 2008b), their mechanical behavior follows the same fundamental principle.

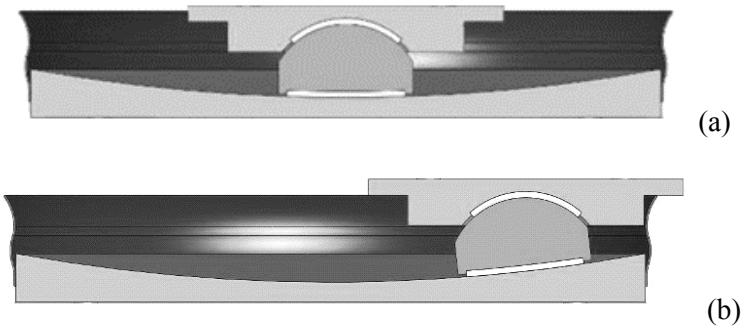

Figure 2. Curved Surface Slider: (a) centered position; (b) deformed position

The large spread of use of the CSS requires of its behavior a detailed knowledge and improved modelling capability under seismic conditions; however its restoring behavior has been never investigated in detail, and in particular, the validity of the Eurocode's provisions has been never checked. The study presents some results from a wide investigation on the restoring capability of Curved Surface Sliders (Quaglini et al., 2017b), aiming at assessing the effect of the non-seismic offset displacement on the actual displacement of the isolation system during an earthquake.

2. PARAMETRIC STUDY

Nonlinear Response History Analyses (NRHAs) were performed on a Single Degree Of Freedom system with an assigned mass of 100 tons, typical of medium-rise residential buildings (Cardone et al. 2015), supported by an isolator element. The numerical model was formulated in OpenSees software, v.2.5.4 (McKenna et al. 2000). The isolation system was modelled using the *SingleFPSimple3d* bearing element available in the software library, with coefficient of friction described as

$$\mu = \mu_{LV} - (\mu_{HV} - \mu_{LV}) \cdot exp(-\alpha \cdot |V|) \quad (5)$$

where constants μ_{LV} and μ_{HV} represent the coefficient of friction at very low and very high velocity, respectively, and α controls the rate of transition from μ_{LV} to μ_{HV} (Constantinou et al. 1991). The restoring stiffness of the isolation system was set as $K_2 = W/R$, where W is the vertical load acting though the isolation system, and R is the radius of curvature of the concave surface, while the elastic stiffness was assumed as $K_1 = 100\ K_2$ (Naim and Kelly 1999).

2.1 Parameters of the CSS

Different values of the main mechanical parameters of the Curved Surface Slider, namely the radius of curvature R and the coefficient of friction μ, were examined in the study, covering the production ranges of current devices on the European market (Table 1).
The five values of radius R corresponded to an undamped isolation period $T_{ISO} = 2\ \pi\ \sqrt{(R/g)}$ ranging from 2.9 to 4.5 seconds, typical for base isolation applications.
To characterize the friction properties, the low velocity friction coefficient μ_{LV} was assigned as independent parameter, while the high velocity coefficient was assumed to count $\mu_{HV} = 2.5\ \mu_{LV}$, and a fixed value $\alpha = 0.0055$ s/mm was assigned to the transition rate parameter (Cardone et al. 2015). Although the variability of the coefficient of friction with axial load and air-temperature (Dolce et al. 2005; Quaglini et al. 2012) was not directly taken in account, it was assumed to be indirectly covered by the examined range of friction coefficients.

Table 1. Parameters of Curved Surface Sliders examined in the study.

parameter	**values**
Radius, R (mm)	2 200 ; 3 000 ; 3 500 ; 4 000 ; 5 000
Coefficient of friction, μ_{LV} (-)	0.02 ; 0.03 ; 0.04 ; 0.05

2.2 Seismic input

One-directional horizontal ground acceleration histories were considered as seismic inputs, while the vertical component of the ground motion was disregarded.
Ground motion records were selected from the Pacific Earthquake Engineering Research Center (PEER) database (http://peer.berkeley.edu/nga). The records were classified according to the custom Pulse Index, PI_k, formulated as the ratio between the time interval $D_{v,T}$ during which the most of the seismic energy is introduced in the structure, and the duration of the quake $D_{v,B}$ (Quaglini et al. 2017b)

$$PI_k = 1 - \frac{D_{v,T}}{D_{v,B}} \tag{6}$$

where $D_{v,T}$ and $D_{v,B}$ are the Trifunac (Trifunac and Brady 1975) and the bracketed (Bolt 1969) durations of the ground motion, respectively; $D_{v,T}$ is calculated as the length of time between the instants when the 5% and the 95% of the energy integral $I_E = \int v_g^2\ dt$ (Anderson and Bertero 1987) is developed (v_g is the ground velocity), and $D_{v,B}$ is calculated as the total time between the first and the last exceeding of 1% of the peak ground velocity. Based on the PI_k rank, the records were classified as "pulse-like" ($PI_k > 0.70$), "weakly-pulse" ($0.40 \le PI_k \le 0.70$), and "non-pulse" ($PI_k < 0.40$).
For each pulse class, the ground motions were further divided depending on the period T_{sv} of the maximum undamped spectral velocity into four ranges, namely $T_{sv} \le 2$ s, 2 s $< T_{sv} \le 3$ s, 3 s $< T_{sv} \le 4$ s, and $T_{sv} > 4$ s, which envelope the isolation periods of the devices examined in the parametric study. It must be underlined that, whereas for pulse-like ground motions T_{sv} coincides with the so-called "pulse period", corresponding to the dominant peak of the velocity response spectrum at which the largest quantity of seismic energy is available, for non-pulse ground motions a significant energy content can be available over a range of periods around T_{sv} depending on the smoothness of the spectrum.
Eventually, two records were selected per each pulse class and period range, for a total of 24 ground motions (Table 2). Though not exhaustive, the set spans the possible ranges of pulsativity and frequency

content of interest for base isolation.

Table 2. Ground motion records and relevant characteristics.

class	Event	PEER file	PI_k (-)	T_{sv} (s)	S.F. (-)
non-pulse	Chi-Chi 1999	RSN3860_CHICHI.05_CHY008N	0.37	0.33	4.7
	Chi-Chi 1999	RSN3858_CHICHI.05_CHY004N	0.34	0.38	10.4
	Chi-Chi 1999	RSN2938_CHICHI.05_CHY016N	2.34	0.29	10.7
	Chi-Chi 1999	RSN3844_CHICHI.03_CHY004N	2.69	0.34	7.7
	Alaska 2002	RSN2102_DENALI_NOAA-90	3.43	0.24	21.4
	Irpinia 1980	RSN297_ITALY_B-BIS270.	3.83	0.39	7.0
	Chi-Chi 1999	RSN3851_CHICHI.04_CHY004W	5.07	0.36	14.0
	Landers 1992	RSN834_LANDERS_ARC262	5.05	0.35	11.0
weakly-pulse	Nahanni 1985	RSN496_NAHANNI_S2330	0.52	0.56	1.9
	Chi-Chi 1999	RSN3846_CHICHI.03_CHY008W	1.52	0.55	9.9
	Cape Mendocino 1992	RSN827_CAPEMEND_FOR000	2.56	0.51	2.6
	Chi-Chi 1999	RSN3844_CHICHI.03_CHY004W	2.90	0.59	5.6
	Cape Mendocino 1992	RSN827_CAPEMEND_FOR090	3.08	0.46	2.7
	Chi-Chi 1999	RSN2695_CHICHI.04_CHY016W	3.82	0.48	13.3
	Alaska 2002	RSN2115_DENALI_PS11-66	5.76	0.47	8.3
	Kocaeli 1999	RSN1170_KOCAELI_MCD090	5.88	0.59	8.8
pulse-like	Morgan Hill 1984	RSN451_MORGAN_CYC285	0.83	0.86	0.5
	Coyote Lake 1979	RSN150_COYOTELK_G06230	1.47	0.84	1.4
	Irpinia 1980	RSN292_ITALY_A-STU270	2.82	0.82	0.8
	Imperial Valley 1979	RSN171_IMPVALL.H_H-EMO270	2.94	0.85	1.0
	Imperial Valley 1979	RSN181_IMPVALL.H_H-E06230	3.40	0.89	0.6
	Imperial Valley 1979	RSN182_IMPVALL.H_H-E07230	3.27	0.85	1.1
	Kocaeli 1999	RSN1148_KOCAELI_ARE090	5.31	0.70	2.0
	Imperial Valley 1979	RSN179_IMPVALL.H_H-E04230	4.08	0.76	0.8

The seismic inputs should generate a variety of peak displacements, in order to investigate the effect of the offset displacement on systems with different re-centering capability. The selected acceleration histories were scaled in amplitude to produce displacements between 5% and 10% of the radius R, which are typical for Curved Surface Sliders according to the current design practice (Calvi et al. 2010). The scale factor (S.F.) adopted for each record is reported in Table 2.

2.3 Offset displacement

The non-seismic displacement of the isolation system $d_{G,i}$ in Equations (2) and (3) includes the effects of permanent actions, of long-term deformations of the superstructure and an appropriate factor (i.e. 50%) of the thermal action (CEN, 2005).
In the study, the non-seismic displacement d_G was expressed in relation to the parameters μ and R, by assigning a reference offset displacement d_O on the order of 1% to 1.6% of R depending on the low

velocity coefficient of friction (Table 3). In this way, the non-seismic displacement was related to the mechanical properties of the Curved Surface Slider, and independent of the actual seismic scenario.

Table 3. Maximum non-seismic displacement d_O assumed in the study.

μ_{LV}	d_O / R
0.02	1.0
0.03	1.2
0.04	1.4
0.05	1.6

Nonlinear Response History Analyses were conducted for the selected ground acceleration histories listed in Table 2. For each combination of isolator's mechanical parameters in accordance with Table 1 and each ground motion, five NRHAs were conducted, examining two non-seismic displacements $d_G = 0.5\ d_O$, and $d_G = 1.0\ d_O$, applied in either direction of motion, plus the reference condition with no offset ($d_G = 0$). A total of 2 400 analyses was performed.

3. RESULTS

The response parameters considered hereinafter are defined in Figure 3: $d_{m,o}$ and d_m are the maximum displacements of the isolation system either moving from the offset displacement d_G, or from the centered position, respectively, while $d_{r,o}$ and d_r are the relevant residual displacements at the end of the motion. The results of the analyses performed are summarized in Figures 4 to 8.

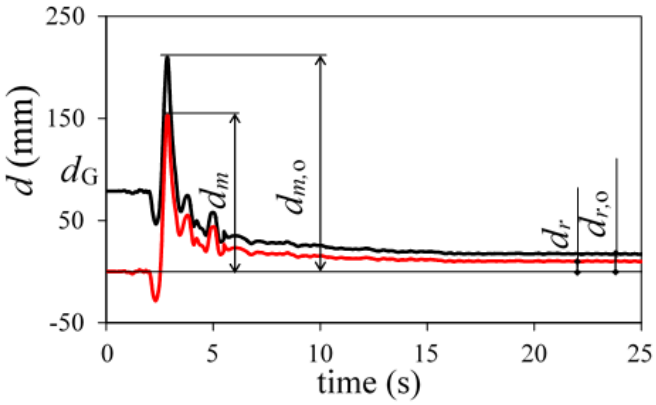

Figure 3. Displacement response histories of the isolation system either with offset (black line) or without offset (red line)

The effect of the non-seismic displacement on the maximum displacement of the isolation system induced by the ground motion is shown in Figure 4, where the ratio between the seismic displacement of the system with offset and the design displacement calculated without offset, $d_{m,o}/d_m$, is plot as a function of the ratio between the design displacement d_m and the maximum residual displacement d_{rm}, expressed as the product of the low velocity friction coefficient times the radius of curvature (Cardone et al. 2015; Quaglini et al. 2017b)

$$d_{rm} = \mu_{LV} \cdot R \tag{7}$$

The definition of d_{rm} given in Equation (7) is consistent with the fact that the system tends to naturally return towards the origin during the coda stage of the ground motion, when the velocity is low.

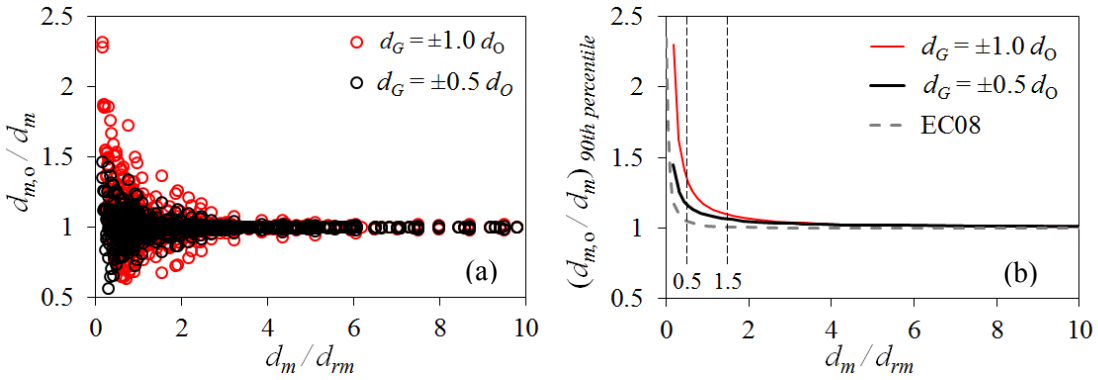

Figure 4. Effect of the non-seismic displacement d_G on the maximum displacement $d_{m,o}$: (a) results of NRHA; (b) comparison (at 90% percentile) with Eurocode (EC08) criterion, Equation (4)

The effect of the non-seismic displacement was negligible for large values of d_m/d_{rm}, whereas in a large number of analyses where d_m/d_{rm} was smaller than 2.5 the non-seismic displacement d_G affected the magnitude of the seismic displacement, producing either an amplification ($d_{m,o}/d_m > 1$) or a decrease ($d_{m,o}/d_m < 1$) with respect to the design value. The effect was larger for larger values of d_G.

By referring to the curves enveloping the 90th percentile of the observed data points shown in Figure 4(b) is it possible to conclude that:

(a) for $d_m/d_{rm} \leq 0.5$, the seismic displacement increased by more than 50% in comparison to the design level when the isolation system was affected from a non-seismic displacement $d_G = d_O$, and by more than 20% when $d_G = 0.5\ d_O$;

(b) for $0.5 < d_m/d_{rm} \leq 1.5$, the effect of the non-seismic displacement was smaller, with maximum increases of the seismic displacement at the 90th percentile between +20% and +50%, but not negligible;

(c) for $d_m/d_{rm} > 1.5$, the effect of the non-seismic displacement became not significant in practice (maximum increase of d_{mo} less than 10% of d_m, irrespective of the value of d_G).

In Figure 4(b) the regression curves are further compared to the criterion recommended by Eurocode 8 for estimating the accumulation of displacement in case of insufficient re-centering capability (Equation (4) in the paper). The difference between the regression curve at the 90th percentile and the code provision became negligible only for $d_m/d_{rm} > 2.5$.

The influence of the friction coefficient and the radius of curvature on the effect of the non-seismic displacement are illustrated in Figures 5(a) and 5(b) respectively. As expected, devices endowed with high coefficient of friction and large radius are more sensitive to an offset displacement because characterized by little re-centering capability; indeed the largest number of analyses showing significant increase of seismic displacement related to such devices. On the contrary, $d_{m,o}/d_m$ ratios close to unity were typically observed for isolators with low friction and/or low radius of curvature.

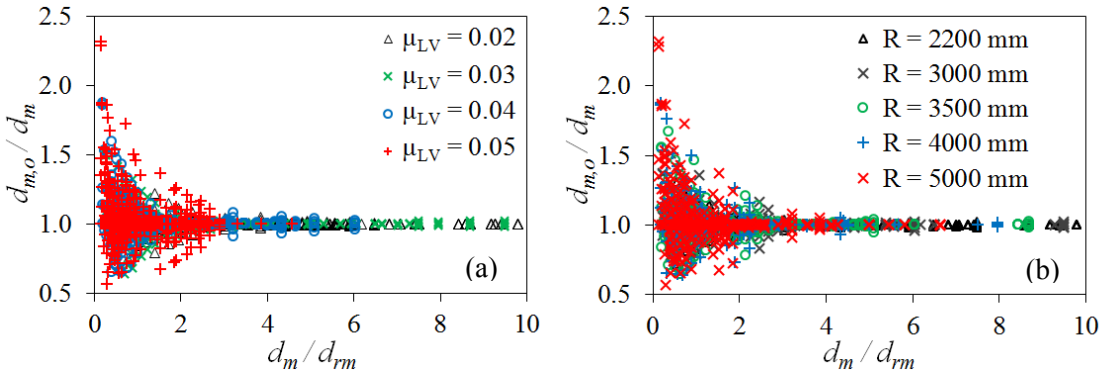

Figure 5. Effect of the non-seismic displacement d_G: (a) influence of coefficient of friction; (b) influence of radius of curvature

The influence of the pulse-like rank of the ground motion is shown in Figure 6. It is evident that, while for no-pulse events the effect of the non-seismic displacement practically disappeared for $d_m/d_{rm} > 0.5$, for pulse-like motions the non-seismic displacement could promote an important increase of the seismic displacement also when $d_m/d_{rm} > 2$.

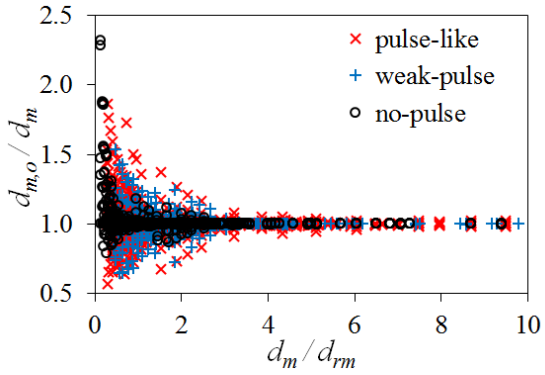

Figure 6. Effect of the non-seismic displacement d_G: influence of pulse rank of the ground motion

To fulfill the non-collapse compliance criterion, the capacity of the isolating devices must not be exceeded at the ultimate limit state. The total displacement $d_{m,o}$ calculated in NRHAs accounting for the effect of both non-seismic and seismic actions is compared in Figure 7 to the displacement capacity in accordance with Eurocode 8, Equation (2) or (3) in the paper:

$$D = max\left\{d_G + \gamma_{IS} \cdot d_m ; d_G + \gamma_{du} \cdot \rho_d \cdot d_m\right\} \tag{8}$$

By accounting for a reliability factor γ_{IS} = 1.5 (recommended value for bridges), the displacement capacity is never exceeded (Figure 7(a)). On the contrary, when γ_{IS} = 1.2 (recommended value for buildings and equivalent structures), Figure 7(b) shows that for a number of analyses where d_m/d_{rm} is between 0.5 and 2.0, the code provision can underestimate by up to 20% the total displacement of the isolating system affected from a non-seismic offset.

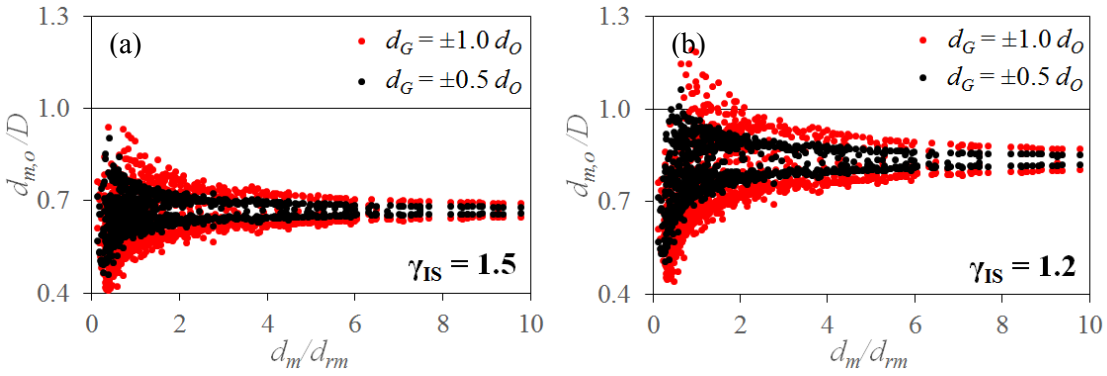

Figure 7. Total seismic displacement with offset ($d_{m.o}$) calculated in NRHAs compared to the horizontal displacement capacity (D) in accordance with the Eurocode: (a) γ_{IS} = 1.5; (b) γ_{IS} = 1.2

A second concern, related to the limitation of damage, is the possible accrual of permanent displacements. To investigate the effect of d_G on the residual displacement at the end of the earthquake, Figure 8(a) illustrates the ratio $d_{r,o}/d_r$ between the residual displacement of the system affected from the non-seismic displacement and the residual displacement of the centered system, as a function of the re-centering parameter d_m/d_{rm}. The effect of d_G disappeared for $d_m/d_{rm} > 2.5$, while for lower values accumulation of permanent displacement occurred in a number of analyses. As a further analysis, in Figure 8(b) the influence of the pulse rank of the ground motion is enlightened. The build up of

permanent displacements typically occurred under pulse-like ground motions for values of d_m/d_{rm} in excess than 0.5 and up to about 2.5, where was negligible for weak-pulse and no-pulse events (for the latter input, displacement accrual was not negligible only for not re-centering systems with $d_m/d_{rm} < 0.5$). A similar behavior was already observed regarding the effect of d_G on the maximum displacement.

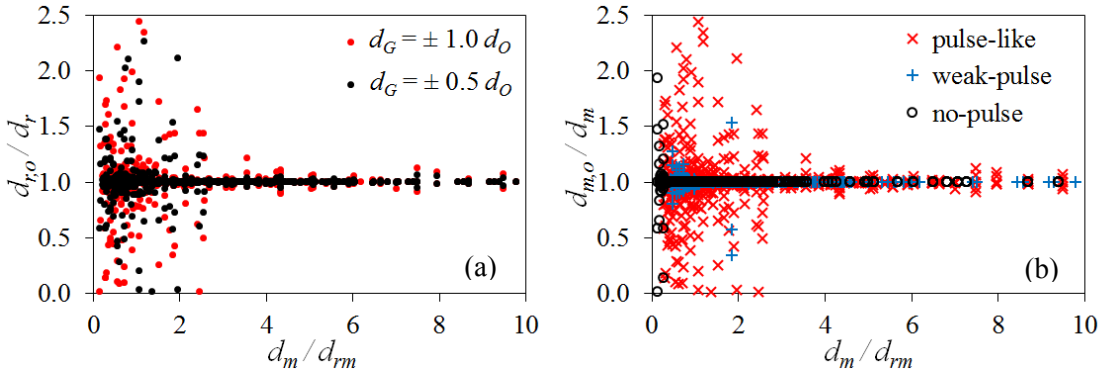

Figure 8. Effect of the non-seismic displacement d_G on the residual displacement $d_{r,o}$: (a) results of NRHA; (b) influence of pulse rank of the ground motion

5. CONCLUSIONS

The effect of the non-seismic displacement d_G on the maximum displacement of an isolation system comprised of Curved Surface Sliders during an earthquake has been investigated in a parametric study. The mechanical properties of the isolating device were changed in order to cover the typical production ranges of the devices today on the European market, while a set of natural ground motions with different frequency and pulse-like content was selected for conductig Nonlinear Response History Analyses.
The main outcomes of the study are summarized in the next points.

(1) the effect of the non-seismic displacement on the total seismic displacement of the isolating system is not negligible for systems with low restoring capability, i.e. when the ratio d_m/d_{rm} is small (where d_m is the design seismic displacement of the system without offset), but it becomes irrelevant when d_m/d_{rm} is greater than 2.5 (or 1.5 considering the 90th percentile of the observed results);

(2) the provision of the Eurocode 8 (CEN 2004, 2005) for determining the ultimate capacity of the isolating devices seems to be not conservative when a reliability factor $\gamma_{IS} = 1.2$ is assumed especially in presence pulse-like ground motions;

(3) when base-isolated structures are located near active faults where pulse-like events are expected to occur (Baker 2007), particular attention should therefore be deserved to the design of the displacement capacity of the isolation system; in such situations it is therefore suggested to adopt the more conservative value $\gamma_{IS} = 1.5$ even in case of buildings. In this regard, it is worth noting that the pulse-like features of the ground motion are not considered by the provisions stated in the code;

(4) the non-seismic displacement affects the residual displacement at the end of the earthquake in a way that is similar to the one observed for the maximum displacement; in presence of small values of d_m/d_{rm}, and under pulse-like ground motions, permanent displacements tend to accumulate;

(5) the criterion $d_m/d_{rm} > 0.5$ recommended by the code seem to over-estimate the re-centering capability of the Curved Surface Sliders; for this type of isolating devices a more conservative figure seems to be appropriate, e.g. $d_m/d_{rm} > 2.5$ as suggested by Cardone et al. (2015).

6. ACKNOWLEDGMENTS

This work has been partially funded by the ReLUIS (Laboratories University Network of Seismic Engineering) Consortium within the ReLUIS/DPC 2014–2018 research program (Research line: Seismic Isolation & Energy Dissipation).

7. REFERENCES

Ancheta TD, Darragh RB, Stewart JP, Seyhan E, Silva WJ, Chiou BSJ, Wooddell KE, Graves RW, Kottke AR, Boore DM, Kishida T, Donahue JL (2013). PEER NGA-West2 Database, *PEER Report 2013/03*, Pacific Earthquake Engineering Research Center (PEER), Berkeley, CA.

Anderson JC, Bertero VV (1987). Uncertainties in establishing design earthquakes. *Journal of Structural Engineering*, 113(8): 1709–1724.

Baker JW. (2007). Quantitative Classification of Near-Fault Ground Motions Using Wavelet Analysis. *Bulletin of the Seismological Society of America*, 97(5): 1486–1501, doi :10.1785/0120060255.

Bolt BA (1969). Duration of strong motion. *Proceedings of the 4th World Conference on Earthquake Engineering*, 13-18 January, Santiago, Chile.

Calvi GM, Pietra D, Moratti M (2010). Criteri per la progettazione di dispositivi di isolamento a pendolo scorrevole. *Progettazione Sismica*, 3(1): 7-30.

CEN (2004). Eurocode 8: Design of structures for earthquake resistance – Part 1: General rules, seismic actions and rules for buildings, EN1998-1:2004, European Committee for Standardization, Brussels.

CEN (2005). Eurocode 8: design of structures for earthquake resistance—Part 2: Bridges, EN1998-2:2005, European Committee for Standardization, Brussels.

Cardone D (2012). Re-centering capability of flag-shaped seismic isolation systems. *Bulletin of Earthquake Engineering*, 10(4): 1267–1284, DOI:10.1007/s10518-012-9343-1.

Cardone D, Gesualdi G, Brancato P (2015). Restoring capability of friction pendulum seismic isolation systems. *Bulletin of Earthquake Engineering*, 13(8): 2449-2480, DOI:10.1007/s10518-014-9719-5.

Cardone D, Gesualdi G (2017). Influence of residual displacements on the design displacement of spherical friction-based isolation systems. *Soil Dynamics and Earthquake Engineering*, 100: 492-503, DOI:10.1016/j.soildyn.2017.07.001.

Carydis P, Castiglioni C, Lekkas E, Kostaki I, Lebesis N, Drei A (2012). The Emilia Romagna, May 2012 earthquake sequence. The influence of the vertical earthquake component and related geoscientific and engineering aspects. *Ingegneria Sismica – International Journal of Earthquake Engineering*, XXIX: 31-58.

Constantinou MC, Mokha A, Reinhorn AM (1991). Teflon bearings in base isolation. II: modeling. *Journal of Structural Engineering*, 116(2): 455-474, DOI:10.1061/(ASCE)0733-9445(1990)116:2(455).

Decanini L, Gavarini C, Mollaioli F (2000). Some remarks on the Umbria-Marche earthquakes of 1997. *European Earthquake Engineering*, 3: 18-48.

Di Sarno L, Elnashai AS, Manfredi G (2011). Assessment of RC columns subjected to horizontal and vertical ground motions recorded during the 2009 L'Aquila (Italy) earthquake. *Engineering Structures*, 33(5): 1514-1535, DOI:10.1016/j.engstruct.2011.01.023.

Di Sarno L, Yenidogan C, Erdik M (2013). Field evidence and numerical investigation of the Mw = 7.1 October 23 Van, Tabanli and the Mw > 5.7 November Earthquakes of 2011. *Bulletin of Earthquake Engineering*, 11(1): 313-346, DOI:10.1007/s10518-012-9417-0.

Dolce M, Cardone D, Croatto F (2005). Frictional behaviour of steel-PTFE interfaces for seismic isolation. *Bulletin of Earthquake Engineering*, 3(1): 75-99, DOI:10.1007/s10518-005-0187-9.

Fenz DM, Constantinou MC (2006). Behaviour of the double concave friction pendulum bearing. *Earthquake Engineering and Structural Dynamics*, 35(11): 1403-1424, DOI: 10.1002/eqe.589.

Fenz DM, Constantinou MC. (2008a). Spherical sliding isolation bearings with adaptive behavior: theory. *Earthquake Engineering and Structural Dynamics*, 37(2): 163-183, DOI: 10.1002/eqe.751.

Fenz DM, Constantinou MC (2008b). Spherical sliding isolation bearings with adaptive behavior: experimental verification. *Earthquake Engineering and Structural Dynamics*, 37(2): 185-205, DOI: 10.1002/eqe.750.

Huang Y, Wu JP, Zhang TZ, Zhang DN (2008). Relocation of the M 8.0 Wenchuan earthquake and its aftershock sequence. *Science in China (Series D)*, 51(12): 1703-1711, DOI: 10.1007/s11430-008-0135-z.

Katsaras CP, Panagiotakos TB, Kolias B (2008). Restoring capability of bilinear hysteretic seismic isolation systems. *Earthquake Engineering and Structural Dynamics*, 37(4): 557-575, DOI: 10.1002/eqe.772.

Martelli A, Clemente P, De Stefano A, Forni M, Salvatori A (2014). Recent development and application of seismic isolation and energy dissipation and conditions for their correct use. *Perspectives on European Earthquake Engineering and Seismology. Volume 1*, Ansal A editor, 449-488, Springer, New York, USA.

McKenna F, Fenves GL, Scott MH (2000). Open System for Earthquake Engineering Simulation. Pacific Earthquake Engineering Research Center (PEER), Berkeley, USA.

Motosaka M, Mitsuji K (2012). Building damage during the 2011 off the Pacific coast of Tohoku Earthquake. *Soils and Foundations*, 52(5): 929-944, DOI:10.1016/j.sandf.2012.11.012.

Naeim F, Kelly JM (1999). Design of Seismic Isolated Structural Structures: From Theory to Practice, John Wiley, New York.

Ponzo FC, Di Cesare A, Leccese G, Nigro D (2017). Shake table testing on restoring capability of double concave friction pendulum seismic isolation systems. *Earthquake Engineering and Structural Dynamics*, 46(14): 2337-2353. DOI:10.1002/eqe.2907.

Quaglini V, Dubini P, Poggi C (2012). Experimental assessment of sliding materials for seismic isolation systems. *Bulletin of Earthquake Engineering*, 10(2): 717-740, DOI:10.1007/s10518-011-9308-9.

Quaglini V, Gandelli E, Dubini P (2017a). Experimental investigation of re-centring capability of curved surface sliders. *Structural Control and Health Monitoring*, 24(2): e1870, DOI:10.1002/stc.1870.

Quaglini V, Gandelli E, Dubini P, Limongelli MP (2017b). Total displacement of curved surface sliders under nonseismic and seismic actions: A parametric study. *Structural Control and Health Monitoring*, 24(12), DOI:10.1002/stc.2031.

Trifunac MD, Brady AG (1975). A study of duration of strong earthquake ground motion. *Bulletin of the Seismological Society of America*, 65(3): 581-626.

Zayas VA, Low SS, Mahin SA (1987). The FPS earthquake protection system: experimental report. *Report No. UCB/EERC-87/01*, Earthquake Engineering Research Center, University of California at Berkeley, CA.

Zayas VA, Low SS, Mahin SA (1990). A simple pendulum technique for achieving seismic isolation. *Earthquake Spectra*, 6(2): 317-333, DOI:10.1193/1.1585573.